

Ultra-efficient degradation of isoquinoline from shale gas wastewater with the diethylamine-ferrate(VI) system: The key role of Fe(IV)/Fe(V) active species

Original

Ultra-efficient degradation of isoquinoline from shale gas wastewater with the diethylamine-ferrate(VI) system: The key role of Fe(IV)/Fe(V) active species / Wang, Y., Chen, X., Chen, L., Cheng, X., Yang, C., Chen, G., Shu, J., Liu, W., Tiraferri, A., Liu, B.. - In: JOURNAL OF HAZARDOUS MATERIALS. - ISSN 0304-3894. - 492:(2025).
[10.1016/j.jhazmat.2025.138215]

Availability:

This version is available at: 11583/3000968 since: 2025-06-16T09:05:57Z

Publisher:

Elsevier B.V.

Published

DOI:10.1016/j.jhazmat.2025.138215

Terms of use:

This article is made available under terms and conditions as specified in the corresponding bibliographic description in the repository

Publisher copyright

Elsevier preprint/submitted version

Preprint (submitted version) of an article published in JOURNAL OF HAZARDOUS MATERIALS © 2025,
<http://doi.org/10.1016/j.jhazmat.2025.138215>

(Article begins on next page)

1 **Removal of organics from shale gas wastewater with**
2 **the diethylamine-ferrate(VI) system: The key role of**
3 **Fe(IV)/Fe(V) active species**

4
5 Ying Wang ^{a,b}, Xin Chen ^{a,b}, Liang Chen ^{a,b}, Xin Cheng ^{a,b}, Chunyan Yang ^{a,b}, Guijing
6 Chen ^{a,b}, Jingyu Shu ^{a,b}, Wen Liu ^c, Alberto Tiraferri ^d, Baicang Liu ^{a,b,*}

7 ^a State Key Laboratory of Hydraulics and Mountain River Engineering, College of
8 Architecture and Environment, Institute for Disaster Management and Reconstruction,
9 Institute of New Energy and Low-Carbon Technology, Sichuan University, Chengdu,
10 Sichuan, 610207, China

11 ^b Yibin Institute of Industrial Technology, Sichuan University Yibin Park, Section 2,
12 Lingang Ave., Cuiping District, Yibin, Sichuan, 644000, China

13 ^c The Key Laboratory of Water and Sediment Sciences, Ministry of Education, College
14 of Environmental Sciences and Engineering, Peking University, Beijing 100871, China

15 ^d Department of Environment, Land and Infrastructure Engineering, Politecnico di
16 Torino, 10129, Turin, Italy

17 Corresponding author: Baicang Liu, E-mail: bcliu@scu.edu.cn; baicangliu@gmail.com

18

19 **Abstract**

20 The radical-based advanced oxidation processes currently in use have limited
21 success in treating typical shale gas wastewaters, due to the interference played by
22 background ions and to the formation of potentially toxic disinfection by-products. A
23 novel, non-radical treatment process combining diethylamine (Di) and ferrate, Fe(VI),
24 was investigated in this study. Compared with Fe(VI) alone, the combination with Di
25 provided enhanced performance in degrading various organic pollutants from shale gas
26 wastewater. The measured removal rates were 99.2%, 76.0%, 10.8%, ~100%, and 80.5%
27 for 2,4-di-tert-butylphenol, 6-methylquinoline, tergitolnp-4, indoline, and isoquinoline
28 (IQL), respectively. The degradation rate constant of the Di/Fe(VI) system was almost
29 3-fold larger than that measured with Fe(VI) alone in the degradation of IQL. A
30 mechanistic investigation suggested that high-valent iron intermediates, namely,
31 Fe(IV)/Fe(V), as well as the ferrate-Di complex, were likely responsible for IQL
32 removal in the Di/Fe(VI) system, while radicals, e.g., HO[•], O₂^{•-}, ¹O₂, did not play a
33 substantial role. The presence of Di promoted the generation of Fe(IV)/Fe(V) by
34 donating electrons. Increasing Fe(VI) dosage, the Di concentration, and decreasing the
35 pH all enhanced the degradation of IQL. The presence of common ions and different
36 matrix compositions did not considerably affect the removal of IQL. Based on the
37 analytical data and on model calculations, three main, possible reaction pathways for
38 IQL degradation were proposed. The Di/Fe(VI) system was also observed to be reactive
39 against other refractory organics, such as diclofenac, carbamazepine, and ciprofloxacin.

40

41 **Keywords:** Potassium ferrate Fe(VI); Diethylamine; Isoquinoline; Shale gas
42 wastewater (SGW); Active high-valent iron species Fe(IV)/Fe(V).

43 **Main**

44 Shale gas has experienced global development as an alternative to conventional
45 energy sources and to improve the resilience of the energy sector¹. However, a large
46 amount of shale gas wastewater (SGW) is produced during its extraction activities,
47 posing a threat to the water environments²⁻⁴. Organic pollutants are the main
48 components of SGW⁵, with composition characterized by high variability and
49 complexity⁶. These pollutants are often harmful and carcinogenic, show poor
50 biodegradability and high toxicity⁷. If not properly managed, they may have severe
51 adverse effects for environmental safety and they pose risks of failure for typical
52 treatment technologies deployed to treat SGW, for example, causing membrane fouling
53 and shorter membrane lifespan⁸.

54 Due to the complex composition of SGW, selecting the appropriate treatment train
55 is particularly important. Methods such as biodegradation^{9,10}, physical treatment^{8,11,12},
56 and chemical oxidation^{7,13} have been applied. Among them, chemical oxidation is
57 particularly attractive, due to its simplicity and efficiency¹⁴. However, the chemical
58 oxidation techniques currently used to treat SGW are largely based on radical-driven
59 (HO^\bullet , $\text{SO}_4^{\bullet-}$) advanced oxidation processes. Radicals generally lack selectivity, thus
60 they are susceptible to scavenging reactions by the coexisting background ions in water,
61 e.g., Cl^- , Br^- , HCO_3^- , and tend to produce disinfection by-products¹⁵.

62 Potassium ferrate (Fe(VI) , $\text{Fe}^{\text{VI}}\text{O}_4^{2-}$), has shown potential as an environmentally
63 friendly and multifunctional oxidant with high oxidation capacity and excellent
64 chemical properties¹⁶⁻¹⁸. The oxidation capacity of Fe(VI) has demonstrated remarkable
65 selectivity, showing resistance to the presence of background impurities in water, thus
66 reducing interference reactions and achieving efficient oxidation of targeted
67 pollutants¹⁹. The Fe(VI) system can transform organic substances, inorganic substances,

68 and heavy metal ions, presenting the functions of oxidation, disinfection, and
69 coagulation, simultaneously²⁰. However, Fe(VI) has the important limitation of
70 undergoing self-decomposition reactions, arguably the most critical barrier for its
71 implementation in water and wastewater treatment²¹. Appropriate activation techniques
72 are needed to minimize self-decomposition pathways, enhance the oxidation capacity
73 of Fe (VI), and broaden its applicability. As reported in the literature, Fe(IV) and Fe(V)
74 species are generally 2 – 6 orders of magnitude more reactive toward organic
75 compounds than Fe(VI)²². As a result, much work has been done to enhance Fe(VI)
76 reactivity to generate Fe(IV)/Fe(V) species through the addition of acids²³,
77 reductants^{19,24}, metal oxides^{18,25,26}, metal ions^{27,28}, silica²⁹, ammonia³⁰, carbonaceous
78 materials^{16,31}, oxidants^{32,33}, and other activators. For example, the addition of ammonia
79 to Fe(VI) oxidation systems has been shown to improve the overall oxidation efficiency.
80 Organic amines are another family of compounds that can activate Fe(VI) and they
81 happen to be key components in shale gas wastewater, since they are commonly added
82 as acid dispersants/surfactants^{34,35}. For instance, the amine components of
83 pharmaceuticals are crucial for their oxidation by Fe(VI) in aquatic environments^{36,37}.
84 Specifically, during the oxidation of sulfonamides, it is the amine parts that dictate the
85 reaction pathways, leading to the formation of oxidized products^{38,39}.

86 In this study, diethylamine (Di) is applied to activate Fe(VI) with the goal of rapid
87 removal of organics in SGW. The specific objectives are: (i) to investigate the removal
88 capacity of various organic pollutants in SGW by combining Di with Fe(VI); (ii) to
89 explore the impact of conditions, including Fe(VI) concentration, Di dosage, solution
90 pH, pollutants concentration, coexisting ions, and water matrix, on the removal
91 performance of pollutants; (iii) to elucidate the presence and role of active species, such
92 as high-valent iron and free radicals; (iv) to propose the possible transformation

93 pathways of organics in the Di/Fe(VI) system; (v) to assess toxicity changes produced
94 by the organics degradation process; (vi) to preliminarily assess the system for practical
95 applications.

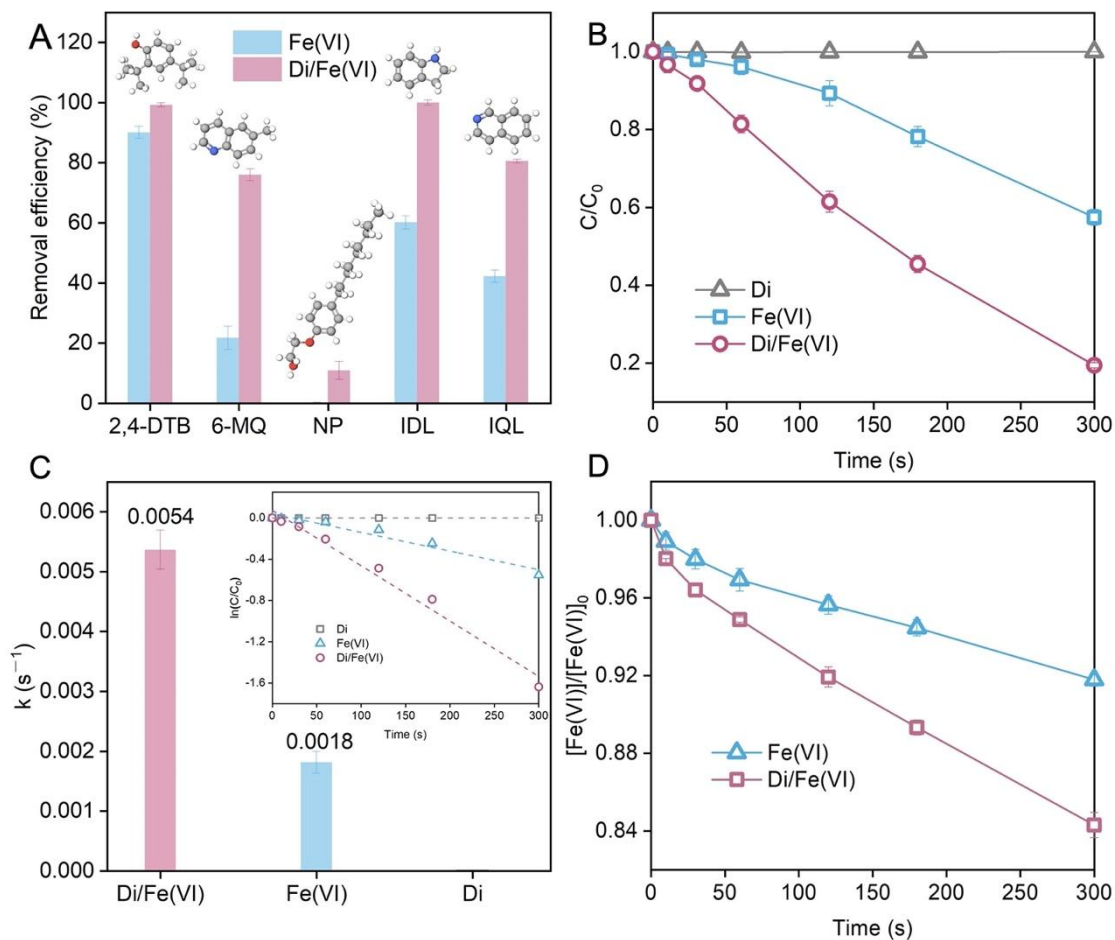
96

97 **Removal of organic pollutants in SWG by the Di/Fe(VI) system**

98 Oxidation tests based on both the Fe(VI) and the Di/Fe(VI) system were initially
99 performed to transform five compounds typically present in SGW, namely, 2,4-di-tert-
100 butylphenol (2,4-DTB), 6-methylquinoline (6-MQ), tergitolnp-4 (NP), indoline (IDL),
101 and isoquinoline (IQL)) (Fig.1a). The Di/Fe(VI) system outperformed the use of Fe(VI)
102 alone in the removal of all five substances, achieving removal rates of over 70% for the
103 majority of them. IQL was selected for additional, detailed experimentation. The data
104 presented in Fig. 1b suggests that the degradation of IQL was negligible (< 1%) by Di
105 alone within 300 s of reaction. The elimination of 42.5% of IQL was observed with
106 Fe(VI) alone, attributed to the formation of Fe-based species , e.g., Fe(IV) and Fe(V),
107 during the Fe(VI) self-decomposition process⁴⁰. When Di and Fe(VI) were co-added
108 into the reaction solution, the IQL removal was substantially enhanced and reached 80.6%
109 within 300 s of reaction

110 As illustrated by the data presented in Fig. 1c, the removal of IQL with both the
111 Fe(VI) and the Di/Fe(VI) was only weakly function of the IQL concentration in the
112 range 4.5-10 μM , suggesting an almost pseudo zero-order kinetics under these
113 conditions. The resulting rate constants were $0.029 \mu\text{M s}^{-1}$ and 0.035 s^{-1} , assuming 0th
114 and 1st order kinetics, respectively, for the Di/Fe(VI) system. Such constants were 3
115 fold higher than that measured with Fe(VI) alone assuming pseudo 0th order kinetics,
116 namely, $0.011 \mu\text{M s}^{-1}$. The results displayed in Fig. 1d indicate that 91.8% and 84.3%
117 residual Fe(VI) was measured in the Fe(VI) and in the Di/Fe(VI) systems, respectively,

118 suggesting that the overall consumption of Fe(VI) was increased in the Di/Fe(VI)
 119 system. In other words, the addition of Di may accelerate the consumption of Fe(VI)
 120 and its reactivity, translating into a higher performance of IQL abatement.



121
 122 Fig.1. Removal efficiency of 2,4-DTB, 6-MQ, NP-9, IND, and IQL in the Fe(VI) and
 123 in the Di/Fe(VI) systems (a); Comparison of the abatement kinetics of IQL in Di alone,
 124 Fe(VI) alone, and in the Di/Fe(VI) systems (b); Data fitting with first-order kinetics and
 125 resulting rate constants of removal IQL by various systems (c); Residual Fe(VI)
 126 concentration as a function of time in the Fe(VI) system and in the Di/Fe(VI) systems
 127 (d). In (b) and (d), lines connecting the data points are provided only as a guide for the
 128 eye. Unless otherwise stated, the reaction conditions were the following: total reaction
 129 time = 300 s; initial contaminant concentration = 10 μ M; pH = 9.0; initial reactant
 130 concentrations, Fe(VI) = xyz, Di = xyz.

131

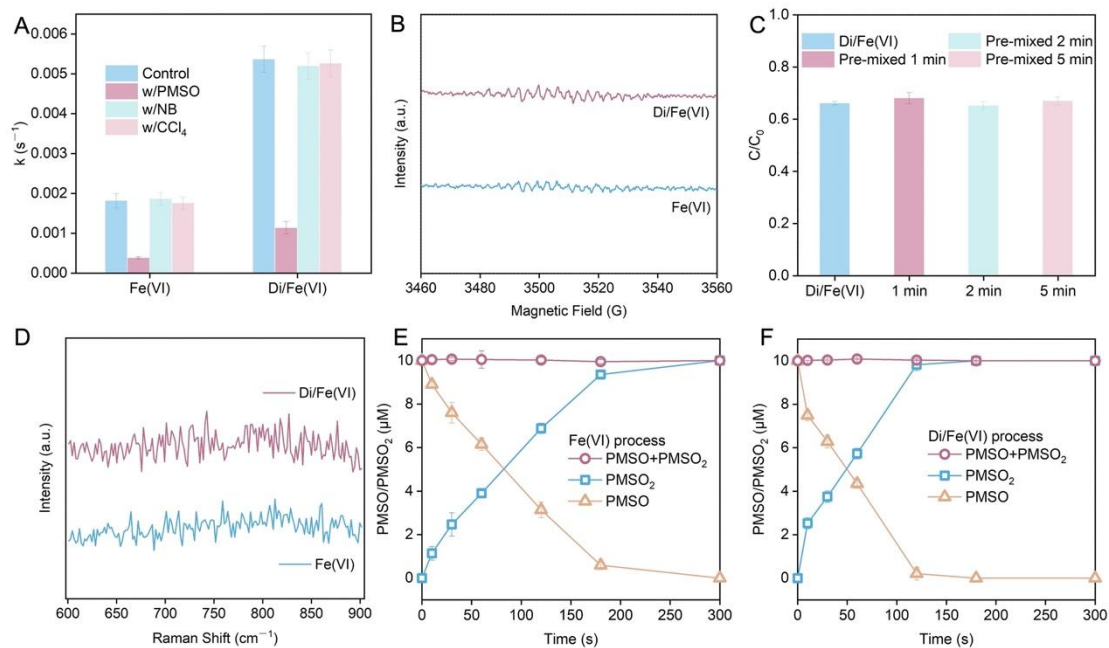
132 **Identification of reactive species**

133 A series of tests was conducted aimed at investigating the possible reactive species
134 contributing to the IQL degradation in the Di/Fe(VI) system, such as hydroxyl radicals
135 (HO^\bullet), superoxide radicals ($\text{O}_2^{\bullet-}$), singlet oxygen ($^1\text{O}_2$), the ferrate-Di complex, and/or
136 high-valent iron species (Fe(IV)/Fe(V))^{26,31,40-43}. The investigation included radical
137 quenching tests, electron paramagnetic resonance (EPR) spectroscopy, pre-mixed
138 experiments, acquisition of Raman spectra, and assays with probe compounds, such as
139 nitrobenzene (NB) and methyl phenyl sulfoxide (PMSO).

140 NB was specifically employed to determine the presence and the possible activity
141 of HO^\bullet because of its pronounced reactivity with this radical, in contrast with its
142 negligible interaction with other reactive species potentially present in the Di/Fe(VI)
143 system^{44,45}. No elimination of NB in the Di/Fe(VI) system was observed (Fig. S2). As
144 indicated by the data plotted in Fig. 2a, the presence of NB had a minor effect on the
145 removal of IQL. Together, these results imply that HO^\bullet was likely not involved in the
146 removal of IQL in the Di/Fe(VI) system. The EPR analysis also corroborated this
147 hypothesis, as no DMPO- HO^\bullet adduct signal was detected (Fig. 2b). CCl_4 was used as
148 the scavenger for $\text{O}_2^{\bullet-}$. Negligible effect on the abatement of IQL was observed in the
149 presence of CCl_4 (Fig. 2a), supporting the contention that $\text{O}_2^{\bullet-}$ was also not a key
150 species responsible for IQL removal. This conclusion was further strengthened by the
151 lack of a reduction response of nitro blue tetrazolium (NBT), a characteristic probe for
152 $\text{O}_2^{\bullet-}$ (Fig. S3)^{46,47}. The potential role of $^1\text{O}_2$ in IQL removal was assessed using a system
153 capable of producing $^1\text{O}_2$ exclusively, namely, visible light illuminated rose bengal
154 (Vis/RB)⁴⁸. The Vis/RB system did not result in the degradation of IQL (Fig. S4),
155 implying that $^1\text{O}_2$ was also not to account for the elimination of IQL. In addition, the

156 role of ferrate-Di complex was ruled out through the results of pre-mixed experiments
157 (Fig. 2c) and Raman spectroscopy (Fig. 2d).

158 With the exclusion of HO[•], O₂^{•-}, ¹O₂, and of the ferrate-Di complex as the reactive
159 species responsible for the elimination of IQL, attention shifted to active iron species,
160 i.e., Fe(IV)/Fe(V). PMSO was used as probe compound to distinguish among different
161 oxidant species through the identification of oxidation products, since Fe(IV)/Fe(V)
162 generally transforms PMSO to the relative sulfone PMSO₂ via a direct one or two
163 electron transfer process, while the radical-based oxidation pathway mainly transforms
164 PMSO into other products, such as hydrolyzed PMSO⁴⁹⁻⁵¹. As indicated by the data
165 shown in Fig.2a, the introduction of PMSO markedly slowed down the degradation of
166 IQL in both Fe(VI) and Di/Fe(VI) systems, acting as an important competing substrate.
167 This result indicates that Fe(IV)/Fe(V) may be principally responsible for the IQL
168 degradation. This claim is supported by the findings presented in Figs. 2e and 2f. Full
169 transformation of PMSO to PMSO₂ was observed in the two systems, reasonably ruling
170 out the possibility of radical involvement in the Di/Fe(VI) system. The results
171 correlated well with the insights gained from the quenching tests, EPR analysis, and
172 probe compound experiments described above. Additionally, in the presence of Di, the
173 degradation of PMSO and the generation of PMSO₂ was significantly faster than that
174 observed in the pure Fe(VI) system. For example, the removal ratio of PMSO at 60 s
175 was 38.5% and 56.5% in the Fe(VI) and in the Di/Fe(VI) system, respectively. The
176 results suggested the role played by Fe(IV) and/or Fe(V) for the enhanced removal rates
177 observed in the Di/Fe(VI) system compared to the Fe(VI) one, the former characterized
178 by stronger oxidation strength^{27,52}.



179

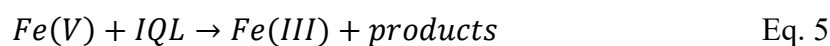
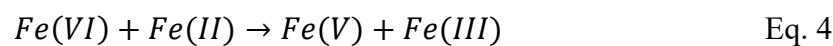
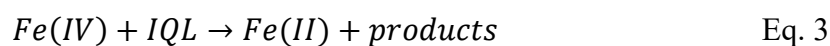
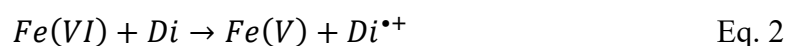
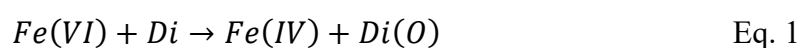
180 Fig.2. Effect of different scavengers and probes on the removal of IQL in the Fe(VI)
 181 and in the Di/Fe(VI) systems (a); EPR detection data of hydroxyl radical (HO•) (b); Pre-
 182 mixed experiments (c); Raman spectra (d); Degradation of PMSO and generation of
 183 PMSO₂ in the Fe(VI) (e) and in the Di/Fe(VI) (f) systems. In (e) and (f), lines
 184 connecting the data points are provided only as a guide for the eye. Unless otherwise
 185 stated, the reaction conditions were the following: total reaction time = 300 s; initial
 186 contaminant concentration = 10 μM; pH = 9.0; initial reactant concentrations, Fe(VI) =
 187 xyz, Di = xyz.

188

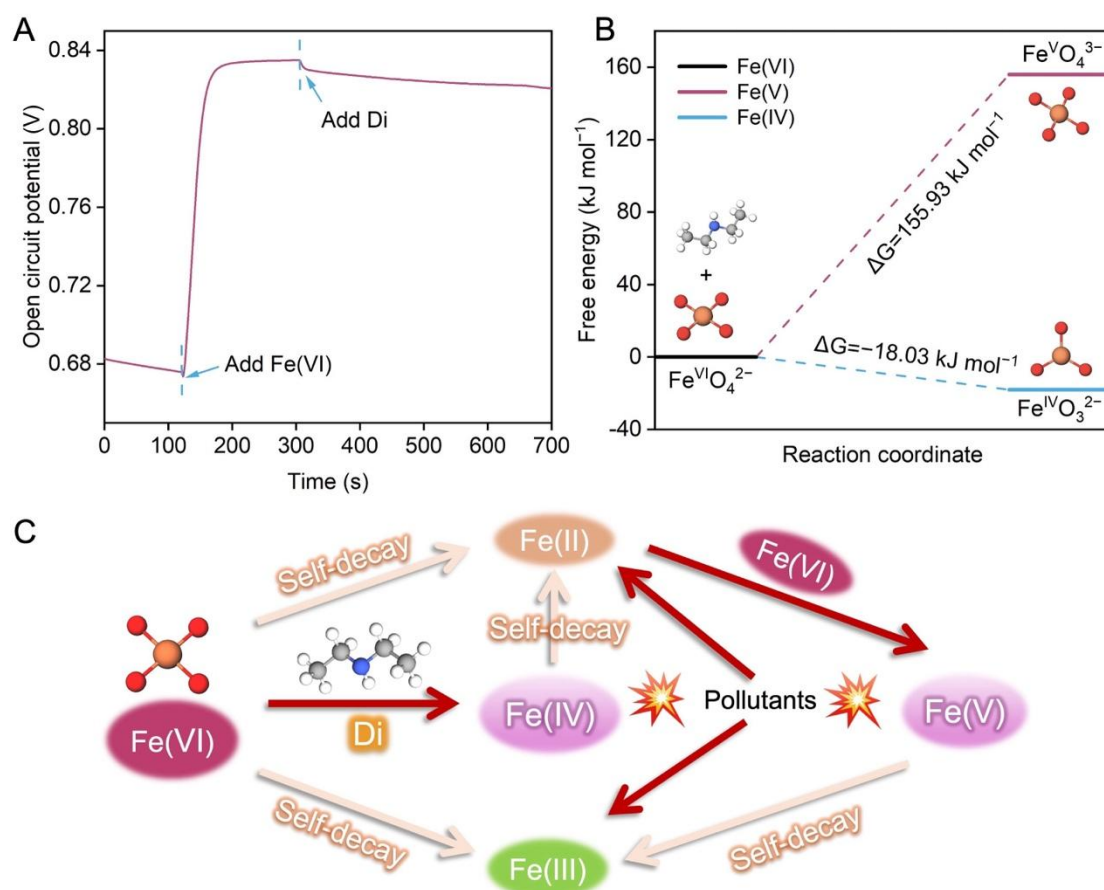
189 Insights into the oxidative species

190 The open circuit potential (OCP) value was measured to evaluate the electron
 191 transfer process, hence elucidate the reaction mechanism between Di and Fe(VI). The
 192 addition of Fe(VI) led to a significant upward trend in voltage, which may be due to the
 193 reduction reaction of Fe(VI) occurring at the electrode (Fig. 3a). After the introduction
 194 of Di, there was a downward trend in voltage, indicating a transfer of electrons in the
 195 Di/Fe(VI) system. Di may in fact provide electrons to assist in the generation of active

196 Fe(IV)/Fe(V) from Fe(VI). Fig. 3b illustrates the calculated thermodynamic values for
197 the conversion from Fe(VI) to Fe(IV) (Eq. 1) or Fe(V) (Eq. 2). According to the
198 calculations, the process of converting Fe(VI) to Fe(V) has a free energy barrier (ΔG)
199 value of $155.9 \text{ kJ mol}^{-1}$, which is an endothermic process, while the conversion to Fe(IV)
200 has a ΔG value of $-18.03 \text{ kJ mol}^{-1}$, indicating an exothermic process. This result implies
201 that generating Fe(IV) is a favorable step for Fe(VI) oxidation and that Fe(V) may not
202 be directly generated by Di activation of Fe(VI). The possible reaction mechanism of
203 the Di/Fe(VI) system is depicted in Fig. 3c. When Fe(VI) reacts with Di, Fe(IV) may
204 form via a two-electron transfer step. These active high-valent Fe species play roles in
205 removing IQL and can yield Fe(II) (Eq. 3)⁴⁰. The newly formed Fe(II) may react with
206 Fe(VI) to produce Fe(V) (Eq. 4). Fe(V) could then also contribute in the effective
207 degradation of target pollutants and generate Fe(III) (Eq. 5). Moreover, a small portion
208 of Fe(IV) or Fe(V) may also react with Di or undergo self-decomposition, consequently
209 generating Fe(II) or Fe(III), respectively. In conclusion, Di may remarkably promote
210 the decomposition of Fe(VI) to generate more Fe(V) and Fe(IV) via a series of reactions,
211 thus enhancing the degradation efficiency of IQL in the Di/Fe(VI) system.



212



213

214 Fig. 3. Open circuit potential (OCP) measurements (a); ΔG of the transformation of
 215 Fe(VI) to Fe(V) and Fe(IV) in the presence of Di (b); Proposed reaction mechanism of
 216 the Di/Fe(VI) system (c).

217

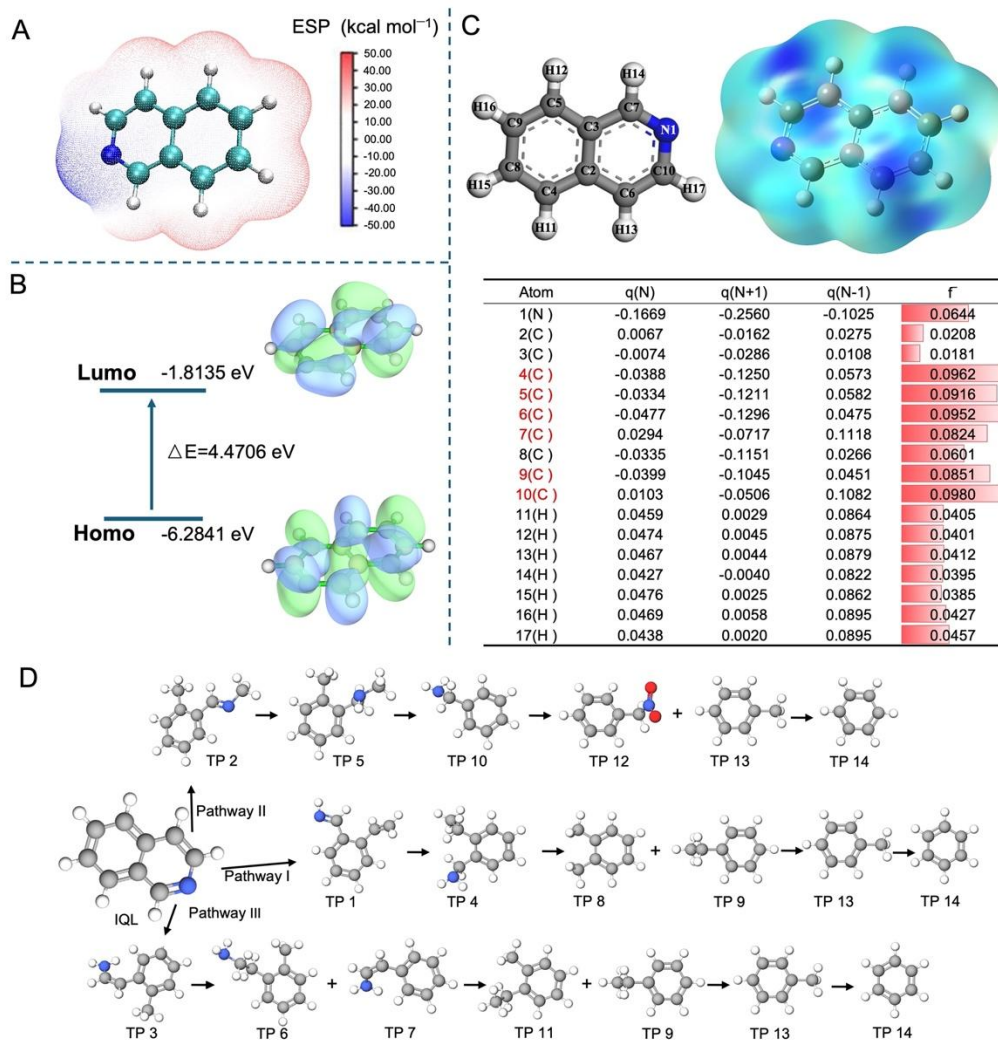
218 **Degradation intermediates and pathway of IQL transformation in the Di/Fe(VI)** 219 **system**

220 The reaction intermediate of IQL transformations in the Di/Fe(VI) system were
 221 identified using GC-MS. IQL, benzene (TP14), methylbenzene (TP13), ethylbenzene
 222 (TP9), o-methylbenzene (TP8), and α -nitrotoluene (TP12) were recognized; the
 223 detailed mass spectral information and MS/MS fragmentation patterns are shown in
 224 [Table S2 and Figs. S5–S10](#). Based on these identified products, three different possible
 225 transformation pathways for the oxidative degradation of IQL by Di/Fe(VI) are

226 proposed, as shown in Fig. 4d. Although GC-MS can determine measurable
227 intermediate products and help propose possible degradation mechanisms, some short-
228 lived products may not be captured, which impairs the determination of comprehensive
229 pathways. Therefore, we further conducted DFT calculations for IQL.

230 Active high-valent Fe species exhibit high reactivity with electron-rich organic
231 compounds. The highest occupied molecular orbital (HOMO) of the IQL molecule (Fig.
232 4b) indicates that electrons can easily escape, making it susceptible to electrophilic
233 attack by high-valent Fe species⁵³. To identify the atoms with the highest likelihood of
234 reactivity, the surface electronegativity was analyzed, since this parameter has an
235 impact on the initial affinity with negatively charged Fe(VI)/Fe(V)/Fe(IV). The bar in
236 Fig. 4a illustrates from blue to red color the distribution of positive and negative
237 electrostatic potentials around IQL, with dark areas representing dense positive charges,
238 associated with better affinity for active high-valent Fe species and higher activation
239 chemical potential⁵⁴. To further understand the active sites and degradation pathways
240 of IQL, the Fukui index representing electrophilic attack (f^-) was calculated (Fig. 4c)⁵⁵.
241 Based on the analysis, C4 ($f^-=0.0962$), C5 ($f^-=0.0916$), C6 ($f^-=0.0952$), C7 ($f^-=0.0824$),
242 C9 ($f^-=0.0851$), and C10 ($f^-=0.0980$), may be the most reactive sites, possessing higher
243 f^- values. Generally, electrophilic reagents prefer to attack areas with high negative
244 electrostatic potential^{24,56}. It is worth noting that, although the estimated f^- values of C4,
245 C5, and C9 are high, they are of positive electrostatic potentials and are also saturated
246 sites. The benzene ring is inherently a robust structure, where the π electron cloud
247 constitutes an extensive conjugated system that permits a uniform distribution of π
248 electrons throughout the entire ring, thereby imparting enhanced stability⁵⁷. As a result,
249 this configuration is highly resistant to attack by high-valent Fe species. The N1 atom
250 has a high negative electrostatic potential (Fig. 4a), which is another reactive site for

251 high-valent Fe species attack. Based on these considerations, N1, C6, C7, C10 are
252 proposed as most likely attack sites for high-valent iron species. The bonds cleavage of
253 C6–C10, C10–N1, and N1–C7 are thermodynamically favorable, which may result in
254 the formation of TP1, TP2, and TP3. The bond population of TPs were calculated to
255 corroborate the transformation pathway (Tables S3–S9). A smaller value of bond
256 population means that the bond is weaker and therefore more prone to breakage. In
257 Pathway I, the C4–C7 and C5–C8 bonds in the TP1 are more vulnerable to breakage.
258 The atoms of N1 and C9 are more vulnerable to high-valent iron species attack to
259 produce TP4. As for TP4, the site of N1 is more resistant to electrophilic species attack,
260 while C7–N1, C8–C9, and C2–C7 bonds are weaker. Thus, the generation of TP8 and
261 TP9 may occur. After that, TP8 and TP9 continue to degrade to generate TP13, followed
262 by TP14. Similarly, Pathways II and III were confirmed. The pathways were similar to
263 what discussed in previous studies^{58,59}.



264

265 Fig. 4. Electrostatic potential (a), HOMO and LUMO distributions (b), molecular
 266 structure and Fukui index (c) of IQL; The proposed mechanisms of IQL degradation in
 267 the Di/Fe(VI) system (d).

268

269 Toxicity assessment

270 Acute and chronic toxicity for fish, daphnid, and green algae were predicted by
 271 Ecological Structure Activity Relationships (ECOSAR) Predictive Model (Fig. S11).
 272 Toxicity for *Daphnia magna*, fathead minnow (*Pimephales promelas*), *Tetrahymena*
 273 *pyriformis*, and oral rat, developmental toxicity, bioaccumulation factors, and
 274 mutagenicity values were predicted with the Toxicity Estimation Software Tool (TEST)
 275 (Fig. S12). According to the Globally Harmonized System of Classification and

276 Labeling of Chemical, hazardous chemicals are categorized into four levels: very toxic
277 ($LC_{50}/ChV \leq 1$ mg/L), toxic ($1 < LC_{50}/ChV \leq 10$ mg/L), harmful ($10 < LC_{50}/ChV \leq$
278 100 mg/L), and not harmful ($LC_{50}/ChV > 100$ mg/L).

279 In terms of acute and chronic toxicity prediction by ECOSAR, among the
280 transformation products, TP12 was non-toxic, and most of other TPs had similar
281 toxicity to the parent substance. For *Daphnia magna*, 4 TPs had similar predicted
282 toxicity to the parent substance, while 10 products were identified as more toxic. For
283 fathead minnow, only 1 TP was predicted as toxic, all others as harmful. For *T.*
284 *pyriformis*, half of the TPs were predicted not harmful, and half as harmful. As for oral
285 rat, almost all TPs exhibited a downward trend of toxicity along the degradation
286 pathway. Overall, the findings suggest the toxicity of most TPs should be lower than
287 that of the parent compound. All the bioaccumulation factors for IQL and TPs were
288 relatively high, indicating a propensity for intracellular accumulation. Five of the TPs
289 exhibited an increase in the bioaccumulation factor, while 7 exhibited a decrease. Note
290 that certain TPs are missing data due to, e.g., complex molecular structures, but these
291 products were relatively harmless to biological and ecological environments¹⁹. Besides,
292 11 products were specifically classified in the group “developmental non-toxicity.”
293 While 4 TPs were found to be mutagenicity positive, 5 TPs were negative. Although
294 the toxicity of these transformation products is not ideal, the strong oxidation behavior
295 of the Di/Fe(VI) system suggests that they may be rapidly mineralized in an
296 appropriately engineered process; see [Fig. S13](#) showing total organic carbon removal
297 as a support for the latter statement.

298 **Effect of conditions on IQL removal in the Di/Fe(VI) system**

299 Oxidant dosage is a significant factor influencing the degradation of contaminants
300 in the chemical oxidation process. The effect of Fe(VI) dosage in the Di/Fe(VI) system

301 was investigated by oxidizing IQL at different concentration of Fe(VI) (0–600 μM). As
302 illustrated in Fig. 5a, when the dosage of Fe(VI) increased from 0 to 500 μM , the
303 removal of IQL substantially accelerated and the final removal percentages showed a
304 consistent increase from 0% to 80.5% with Fe(VI) concentrations, in tests with duration
305 of 300 s. In contrast, when the Fe(VI) concentration was further increased from 500 μM
306 to 600 μM , the overall removal efficiency showed modest increase (from 80.5% to
307 84.0%). As the dosage of Fe(VI) increased, more active iron species were produced.
308 However, there seemed to be a critical point above which an increase in Fe(VI) dosage
309 no longer enhanced the degradation efficiency of IQL and instead the reaction became
310 limited by the dosage of Di. Additionally, excessive levels of Fe(VI) may prompt side
311 reactions that promote Fe(VI) consumption⁶⁰. After considering both the efficacy of
312 IQL removal and the costs involved in the process, a concentration of 500 μM Fe(VI)
313 was determined to be the optimal dosage for the Di/Fe(VI) system for the specific
314 conditions considered in this study.

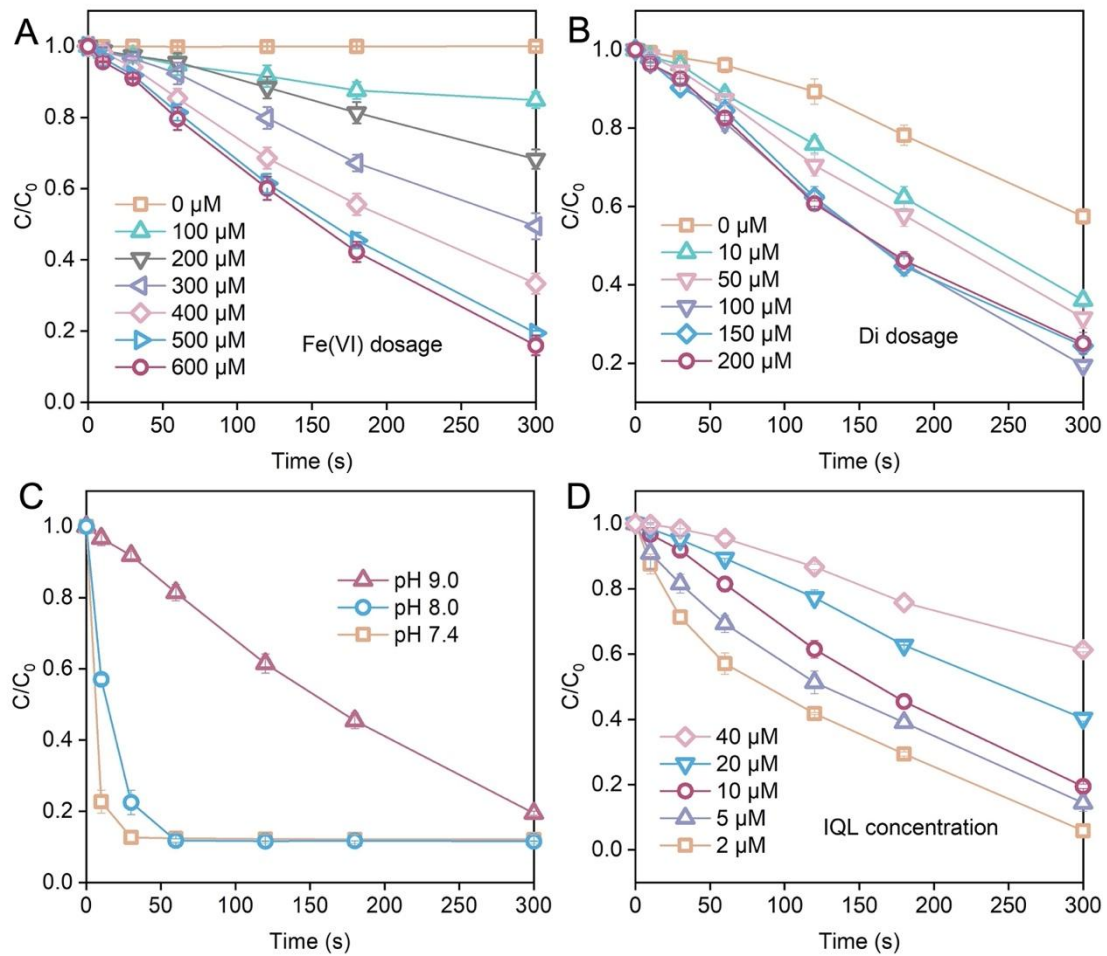
315 The effect of Di dosage on the elimination of IQL in Di/Fe(VI) system was thus
316 investigated. As depicted in Fig. 5b, when the dosage of Di increased from 0 to 200 μM ,
317 the removal of IQL accelerated. However, the overall removal extent did not increase
318 consistently; in detail, the removal extent increased remarkably from roughly 40% to
319 62% by only increasing Di concentration from 0 to 10 μM , but subsequent step
320 increments from 10 μM to 100 μM only brought about an increase up to ~85% of the
321 overall removal. Actually, a slight decline of IQL removal was observed with further
322 increase of Di dosage to 200 μM . This phenomenon could be attributed to the following
323 reasons: (i) the removal of IQL decreased because of the limiting concentration of
324 Fe(VI); (ii) the addition of excess Di led to the predominance of reactions that resulted
325 in the overall decrease of the concentration of Fe(IV) and Fe(V). Based on the results,

326 a dosage of 100 μM Di was chosen as the optimal one for the Di/Fe(VI) system under
327 the conditions investigated in this study.

328 The pH value also stands as an important determinant of the performance of
329 oxidants like Fe(VI) as pointed out, for example, by Tian and colleagues¹⁸. The findings
330 of the investigation on the effect of pH are graphically depicted in Fig. 5c. When the
331 solution pH was 7.4 and 8.0, there was little or no difference in the final elimination
332 efficiency of IQL within 300 s, with measured removal ratios of around 87.9 % and
333 88.4%, respectively. However, there was a significant difference when the solution pH
334 was 9.0, at which the reaction rate was notably slower. This deceleration may be
335 attributed to the stability of Fe(VI): as the pH climbs, so does the stability of Fe(VI),
336 resulting in a less reactive state, consistent with the previous studies^{18,52,61}.

337 The degradation of IQL by Di/Fe(VI) system at an initial IQL concentration in the
338 range 2 – 40 μM was investigated (Fig. 5d). An overall lower removal efficacy was
339 observed with an increasing amount of IQL. Note that these data also allow expanding
340 the discussion around reaction kinetics compared to that mentioned above. The kinetics
341 rate did increase slightly with IQL concentration in the low spectrum of concentrations,
342 implying a weak 1st order rate. The resulting 1st rate constant was 0.0052 s^{-1} in the range
343 0 to ~ 5 μM of IQL. Above this point, the kinetics rate quickly became nearly constant
344 with IQL concentration, or did not show an obvious trend, and may be described by a
345 0th order constant equal to 0.039 $\mu\text{M s}^{-1}$. Note that this result is consistent with the
346 above discussion about kinetics based on the data presented in Fig. 1C. Indeed, such 0th
347 order constant extracted from a concentration range between 0 and 40 μM of IQL is
348 similar to that presented above and based only on the test performed with initial IQL
349 concentration of 10 μM . As of now, it is not clear whether the observed slowing down
350 of kinetics is due to an inhibitory effect of IQL substrate at high concentrations, and/or

351 to an insufficient reactant/substrate ratio under such conditions. Overall, this kinetics
 352 behavior translates into a lower relative removal efficiency at any fixed time when
 353 starting from higher contaminant concentrations, and it suggest that the reaction time
 354 required to achieve a certain removal efficiency may increase considerably with the
 355 initial IQL concentration.



356
 357 Fig. 5. Effect of Fe(VI) dosage(a), Di dosage (b), solution pH (c), and IQL concentration
 358 (d) on the relative removal efficiency of IQL by Di/Fe(VI) system, plotted as a function
 359 of reaction time. Lines connecting the data points are provided only as a guide for the
 360 eye. Unless otherwise stated, the reaction conditions were the following: initial
 361 contaminant concentration = 10 μM ; pH = 9.0; initial reactant concentrations, Fe(VI) =
 362 xyz, Di = xyz.

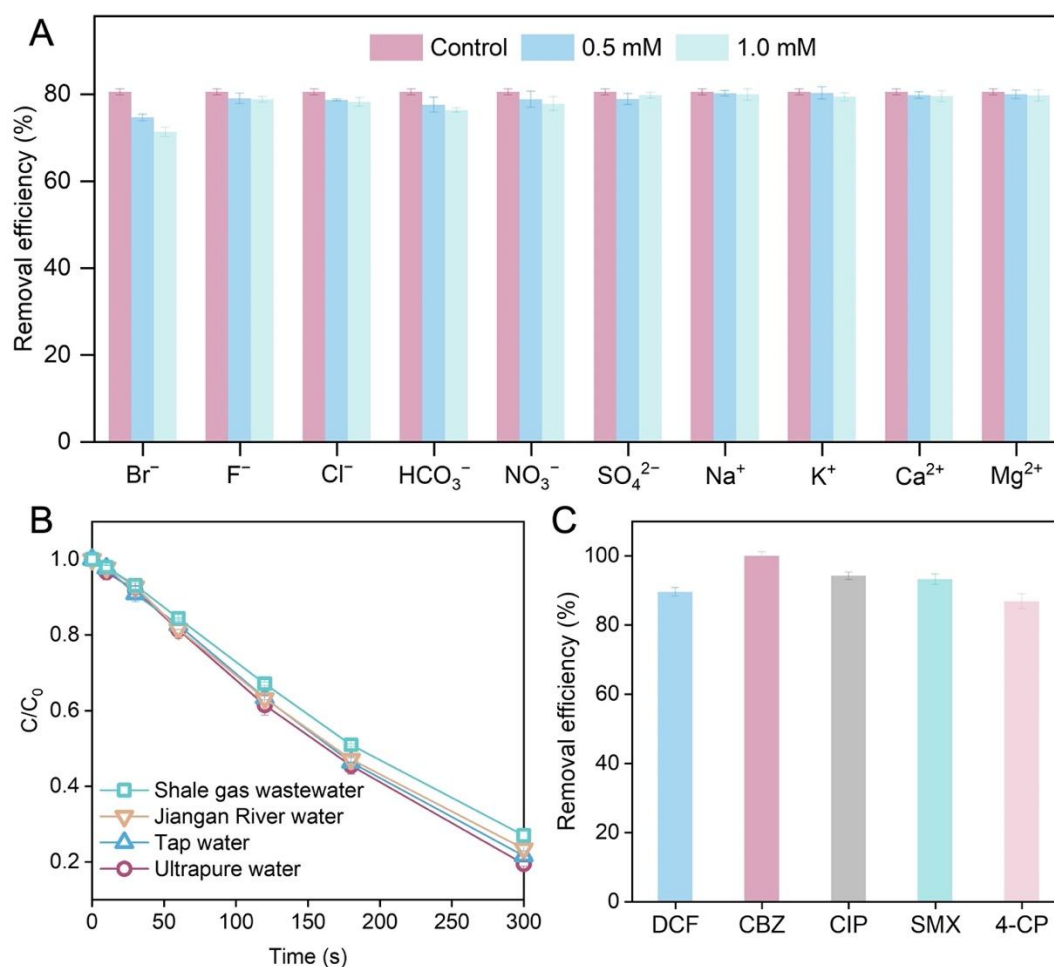
363

364 **Considerations for practical application of the Di/Fe(VI) system**

365 Several common ions typically present in shale gas wastewater matrices (Br^- , Cl^- ,
366 F^- , HCO_3^- , NO_3^- , SO_4^{2-} , Na^+ , K^+ , Ca^{2+} , and Mg^{2+})⁶² were investigated to evaluate their
367 effects on the oxidation performance of the Di/Fe(VI) system. As presented in Fig. 6a,
368 the presence of Br^- had a slight effect on the removal of IQL. As the Br^- concentration
369 gradually increased, the removal rate of IQL gradually decreased. When the
370 concentration of Br^- was 0.5 mM and 1.0 mM, the removal efficiency of IQL decreased
371 to 74.7% and 71.3%, respectively. This result may be explained with the help of a
372 previous study by Li and colleagues⁴⁵, who explored the formation of bromate (BrO_3^-)
373 in the co-presence of Fe(VI) and Br^- , the study suggesting that the formation of BrO_3^-
374 was due to the oxidation of OBr^- by Fe(VI) and Fe(V)/Fe(IV), which may have thus
375 reduced the production and availability of Fe(IV)/Fe(V) for IQL removal. Apart from
376 Br^- , the presence of the other ions at concentrations of 0.5 and 1.0 mM did not
377 demonstrate substantial inhibitory effects. Overall, the removal efficiencies were
378 always above 70%, despite the presence of potentially competing ions, which may be
379 considered a largely inconsequential effect of ion composition at least in concentrations
380 equal or below 1 mM, pointing out the potential of this system for a more selective
381 oxidation strategy compared to current options.

382 To assess the feasibility of the Di/Fe(VI) system in different water matrices,
383 experiments were also conducted using SGW, tap water, ultrapure water, and river
384 water. As shown in Fig. 6b, IQL removal in ultrapure water, tap water, and water from
385 the Jiangan river water were practically the same, while the test performed in SGW
386 showed a minor inhibition role on IQL removal, maybe due to the presence of complex
387 organic substances, which may compete with IQL for Fe(VI)⁵. Finally, the oxidation
388 performance of the Di/Fe(VI) system was also preliminarily tested for the removal of

389 other pollutants, including DCF, CBZ, CIP, SMX, and 4-CP. As presented in Fig. 6c,
 390 the removal efficiencies were all higher than 80% within 300 s of experiment.



391

392 Fig. 6. Effect on the IQL removal performance in the Di/Fe(VI) system of the presence
 393 of F⁻, Br⁻, Cl⁻, HCO₃⁻, NO₃⁻, SO₄²⁻, Na⁺, K⁺, Ca²⁺, and Mg²⁺ (a), of the water matrix
 394 (b). In (b), lines connecting the data points are provided only as a guide for the eye.
 395 Removal efficiency of diclofenac (DCF), carbamazepine (CBZ), ciprofloxacin (CIP),
 396 sulfamethoxazole (SMX), and 4-chlorophenol (4-CP) in Di/Fe(VI) system (c). Unless
 397 otherwise stated, the reaction conditions were the following: total reaction time = 300
 398 s; initial contaminant concentration = 10 μM; pH = 9.0; initial reactant concentrations,
 399 Fe(VI) = xyz, Di = xyz.

400

401 **Conclusions**

402 In this study, diethylamine was observed to be an efficient activator of Fe(VI) to
403 enhance the removal of organic pollutants in shale gas wastewater. Under conditions
404 consisting of pH value equal to 9.0, Fe(VI) dosage of 500 μM , Di dosage of 100 μM ,
405 and initial isoquinoline (IQL) concentration of 10 μM , the degradation rate reached 80.6%
406 within 300 s. The degradation of IQL in the Fe(VI) and in the Di/Fe(VI) systems was
407 found to fit a pseudo first-order kinetic model at low contaminant concentration and
408 near zero-order kinetics at concentrations $> \sim 5 \mu\text{M}$, with the rate constant observed in
409 Di/Fe(VI) system almost 3 fold larger than that measured with Fe(VI) alone. Fe(IV)
410 and Fe(V) were identified as the primary active species for IQL removal in the Di/Fe(VI)
411 system, and the presence of Di promoted the generation of Fe(IV)/Fe(V). Based on the
412 intermediates identified with GC-MS measurements and density functional theory
413 calculations (Fukui indices and bond populations), three oxidation pathways of IQL by
414 Di/Fe(VI) were proposed. The results of coexisting ions and water matrix indicated no
415 substantial effect of water composition for ionic concentrations $\leq 1 \text{ mM}$, suggesting
416 that the Di/Fe(VI) system is a potentially stable and effective treatment method even
417 for matrices with complex inorganic composition. The Di/Fe(VI) system was also
418 effective in the removal of other organic molecules, namely, diclofenac, carbamazepine,
419 ciprofloxacin, sulfamethoxazole, and 4-chlorophenol, implying a wide range of
420 applicability.

421

422 **Methods**

423 **Chemicals and reagents**

424 In this work, potassium ferrate (K_2FeO_4 , Fe(VI)) was synthesized based on a wet
425 chemical oxidation method according to Thompsons' study⁶³; relevant information is
426 given in [Text S1](#) of the Supporting Information (SI). Shale gas wastewater was sourced

427 from Nanchuan, Chongqing. Detailed descriptions of the chemicals and reagents are
428 provided in [Text S2](#).

429 Experimental procedures

430 All experiments were conducted in 150 mL glass beaker containing 100 mL
431 reaction solution and initiated by simultaneously adding the specific amount of Di and
432 solid Fe(VI) while stirring at 300 r min^{-1} with a magnetic stirrer. Unless otherwise
433 specified, solution pH was maintained at pH 9.0 by addition of 10 mM borate buffer,
434 and the fluctuation of reaction pH was controlled in ± 0.5 units. As needed, additional
435 acid or alkali was added to adjust the solution pH. At scheduled time interval, an aliquot
436 of 1 mL solution was sampled and mixed with excess $\text{NH}_2\text{OH}\cdot\text{HCl}$ to terminate the
437 reactions (Huang et al., 2021; Wang et al., 2023). Then, the samples were filtered
438 through a $0.22 \mu\text{m}$ PTFE membrane into 2 mL vials before analysis. All the oxidation
439 experiments were independently repeated at least twice, and the obtained average
440 values and related standard deviations are presented. Pre-mixed experimental
441 procedures are described in [Text S3](#).

442 Analytical methods

443 The pH value of the solution was determined with a regularly calibrated pH meter
444 (Mettler Toledo FE-28, USA). The concentrations of pollutants (e.g., 2,4-DTB, 6-MQ,
445 NP, IDL, IQL, NB, PMSO, and PMSO_2) were monitored with a ultra-performance
446 liquid chromatography apparatus (Shimadzu LC-16, Japan), equipped with a UV
447 detector and Shim-pack GIST C18 ($5 \mu\text{m}$, $4.6 \times 250 \text{ mm}$); additional details are
448 summarized in [Text S4](#) and [Table S1](#). Absorbance measurement were conducted with a
449 AquaMate 8000 UV-vis spectrometer (USA). The desired Fe(VI) concentrations were
450 quantified at a wavelength of 510 nm with a molar absorption coefficient of $\epsilon_{510 \text{ nm}} =$
451 $1150 \text{ M}^{-1} \text{ cm}^{-1}$ ⁶⁴. Detailed experimental procedures for measuring residual Fe(VI) are

452 presented in [Text S5](#). Other analytical methods are described in [Texts S6–S12](#).

453 Density functional theory calculations

454 To predict the most likely active reaction sites of IQL, DFT calculations were
455 performed via Gaussian software. The IQL geometry optimization was conducted using
456 the Gaussian 16 software with the B3LYP-D3/6–311+G(d) method. Detailed
457 information is presented in [Text S13](#).

458

459 **Data availability**

460 All data are presented in the article and its Supplementary Information. Source data are
461 provided with this paper.

462

463 **References**

- 464 1. Kerr, R. A. Natural Gas From Shale Bursts Onto the Scene. *Science* **328**, 1624–
465 1626 (2010).
- 466 2. Bonetti, P., Leuz, C. & Michelon, G. Large-sample evidence on the impact of
467 unconventional oil and gas development on surface waters. *Science* **373**, 896–902
468 (2021).
- 469 3. Vidic, R. D., Brantley, S. L., Vandenbossche, J. M., Yoxtheimer, D. & Abad, J. D.
470 Impact of Shale Gas Development on Regional Water Quality. *Science* **340**, 1235009
471 (2013).
- 472 4. Yang, H., Flower, R. J. & Thompson, J. R. Shale-Gas Plans Threaten China’s
473 Water Resources. *Science* **340**, 1288–1288 (2013).
- 474 5. Butkovskiy, A., Bruning, H., Kools, S. A. E., Rijnaarts, H. H. M. & Van Wezel, A.
475 P. Organic Pollutants in Shale Gas Flowback and Produced Waters: Identification,
476 Potential Ecological Impact, and Implications for Treatment Strategies. *Environ. Sci.*
477 *Technol.* **51**, 4740–4754 (2017).
- 478 6. Tao, Z., Liu, C., He, Q., Chang, H. & Ma, J. Detection and treatment of organic
479 matters in hydraulic fracturing wastewater from shale gas extraction: A critical review.
480 *Sci. Total Environ.* **824**, 153887 (2022).
- 481 7. Chen, X., Zhao, G., Yang, Z. & Li, Q. Molecular comparison of organic matter
482 removal from shale gas flowback wastewater: Ozonation versus Fenton process. *Sci.*
483 *Total Environ.* **905**, 167147 (2023).
- 484 8. Liu, Y. *et al.* Green aerogel adsorbent for removal of organic compounds in shale
485 gas wastewater: High-performance tuning and adsorption mechanism. *Chem. Eng. J.*
486 **416**, 129100 (2021).
- 487 9. Hanson, A. J. *et al.* High total dissolved solids in shale gas wastewater inhibit

- 488 biodegradation of alkyl and nonylphenol ethoxylate surfactants. *Sci. Total Environ.* **668**,
489 1094–1103 (2019).
- 490 10. Sun, Y., Huang, L., Lai, C., Li, H. & Yang, P. Removal of organics from shale gas
491 fracturing flowback fluid using expanded granular sludge bed and moving bed biofilm
492 reactor. *Environ. Technol.* **42**, 3736–3746 (2021).
- 493 11. Wang, B., Xiong, M., Shi, B., Li, Z. & Zhang, H. Treatment of shale gas flowback
494 water by adsorption on carbon- nanotube-nested diatomite adsorbent. *J. Water Process
495 Eng.* **42**, 102074 (2021).
- 496 12. Ye, J. *et al.* Removal of 6-methylquinoline from shale gas wastewater using
497 electrochemical carbon nanotubes filter. *Chemosphere* **359**, 142259 (2024).
- 498 13. Tang, P. *et al.* Organics removal from shale gas wastewater by pre-oxidation
499 combined with biologically active filtration. *Water Res.* **196**, 117041 (2021).
- 500 14. Tan, B., He, Z., Fang, Y. & Zhu, L. Removal of organic pollutants in shale gas
501 fracturing flowback and produced water: A review. *Sci. Total Environ.* **883**, 163478
502 (2023).
- 503 15. Lee, J., Gunten, U. V. & Kim, J. H. Persulfate-based Advanced Oxidation: Critical
504 Assessment of Opportunities and Roadblocks. *Environ. Sci. Technol.* **54**, 3064–3081
505 (2020).
- 506 16. Deng, Z. *et al.* Highly efficient activation of ferrate (VI) via corncob biochar
507 assisted by electrochemistry for the removal of sulfamethoxazole from water. *Chem.
508 Eng. J.* **484**, 149479 (2024).
- 509 17. Liu, M. *et al.* Insights into manganese(VII) enhanced oxidation of benzophenone-
510 8 by ferrate(VI): Mechanism and transformation products. *Water Res.* **238**, 120034
511 (2023).
- 512 18. Tian, B., Wu, N., Liu, M., Wang, Z. & Qu, R. Promoting Effect of Silver Oxide

- 513 Nanoparticles on the Oxidation of Bisphenol B by Ferrate(VI). *Environ. Sci. Technol.*
514 **57**, 15715–15724 (2023).
- 515 19. Chen, K. *et al.* New insights into degradation of emerging contaminants by
516 S(IV)/Fe(VI) system in neutral water: Performance enhancement, reaction mechanisms
517 and toxicity assessment. *Sep. Purif. Technol.* **328**, 125112 (2024).
- 518 20. Wang, J. *et al.* Oxidation of selected fluoroquinolones by ferrate(VI) in water:
519 Kinetics, mechanism, effects of constituents, and reaction pathways. *Environ. Res.* **243**,
520 117845 (2024).
- 521 21. Deng, Y. & Abdel-Shafy, H. I. Barriers to Ferrate(VI) Application in Water and
522 Wastewater Treatment. *Environ. Sci. Technol.* **58**, 3057–3060 (2024).
- 523 22. Sharma, V. K. *et al.* Reactive High-Valent Iron Intermediates in Enhancing
524 Treatment of Water by Ferrate. *Environ. Sci. Technol.* **56**, 30–47 (2022).
- 525 23. Manoli, K. *et al.* Pharmaceuticals and pesticides in secondary effluent wastewater:
526 Identification and enhanced removal by acid-activated ferrate(VI). *Water Res.* **148**,
527 272–280 (2019).
- 528 24. Zhao, Z. *et al.* New insights into the Ferrate-Sulfite system for the degradation of
529 polycyclic aromatic Hydrocarbons: A dual role for sulfite. *Chem. Eng. J.* **477**, 147157
530 (2023).
- 531 25. Shu, J. *et al.* Insight into the mechanism of ferrate(VI) activation by mineral zincite
532 for carbamazepine degradation: Role of Fe(V) species and free radical induction. *Chem.*
533 *Eng. J.* **473**, 145360 (2023).
- 534 26. Wu, Y. *et al.* Enhanced Oxidation of Organic Compounds by the Ferrihydrite–
535 Ferrate System: The Role of Intramolecular Electron Transfer and Intermediate Iron
536 Species. *Environ. Sci. Technol.* (2023) doi:10.1021/acs.est.3c05798.
- 537 27. Feng, M., Jinadatha, C., McDonald, T. J. & Sharma, V. K. Accelerated Oxidation

538 of Organic Contaminants by Ferrate(VI): The Overlooked Role of Reducing Additives.
539 *Environ. Sci. Technol.* **52**, 11319–11327 (2018).

540 28. Zhang, X. *et al.* Effect of Metal Ions on Oxidation of Micropollutants by
541 Ferrate(VI): Enhancing Role of FeIV Species. *Environ. Sci. Technol.* **55**, 623–633
542 (2021).

543 29. Manoli, K., Nakhla, G., Feng, M., Sharma, V. K. & Ray, A. K. Silica gel-enhanced
544 oxidation of caffeine by ferrate(VI). *Chem. Eng. J.* **330**, 987–994 (2017).

545 30. Rougé, V., Nguyen, P. T. T. H., Allard, S. & Lee, Y. Reaction of Amino Acids
546 with Ferrate(VI): Impact of the Carboxylic Group on the Primary Amine Oxidation
547 Kinetics and Mechanism. *Environ. Sci. Technol.* acs.est.2c03319 (2022)
548 doi:10.1021/acs.est.2c03319.

549 31. Wang, Y. *et al.* Enhanced ferrate(VI) oxidation of organic pollutants through direct
550 electron transfer. *Water Res.* **244**, 120506 (2023).

551 32. Niu, L. *et al.* Ferrate(VI)/Periodate System: Synergistic and Rapid Oxidation of
552 Micropollutants via Periodate/Iodate-Modulated Fe(IV)/Fe(V) Intermediates. *Environ.*
553 *Sci. Technol.* (2023) doi:10.1021/acs.est.2c08965.

554 33. Wang, Z. *et al.* Ferrate(VI)/percarbonate for the oxidation of micropollutants:
555 Interactive activation and release of low-concentration hydrogen peroxide for efficient
556 electron utilization. *J. Hazard. Mater.* **469**, 134029 (2024).

557 34. Thacker, J. B., Carlton, D. D., Hildenbrand, Z. L., Kadjo, A. F. & Schug, K. A.
558 Chemical Analysis of Wastewater from Unconventional Drilling Operations. *Water* **7**,
559 1568–1579 (2015).

560 35. Baum, J. C., Feng, M., Guo, B., Huang, C.-H. & Sharma, V. K. Generation of
561 Iron(IV) in the Oxidation of Amines by Ferrate(VI): Theoretical Insight and
562 Implications in Oxidizing Pharmaceuticals. *ACS EST Water* **1**, 1932–1940 (2021).

- 563 36. Liu, H. *et al.* Oxidative degradation of chlorpyrifos using ferrate(VI): Kinetics and
564 reaction mechanism. *Ecotoxicol. Environ. Saf.* **170**, 259–266 (2019).
- 565 37. Luo, C., Feng, M., Sharma, V. K. & Huang, C.-H. Oxidation of Pharmaceuticals
566 by Ferrate(VI) in Hydrolyzed Urine: Effects of Major Inorganic Constituents. *Environ.*
567 *Sci. Technol.* **53**, 5272–5281 (2019).
- 568 38. Feng, M. *et al.* Oxidation of Sulfonamide Antibiotics of Six-Membered
569 Heterocyclic Moiety by Ferrate(VI): Kinetics and Mechanistic Insight into SO₂
570 Extrusion. *Environ. Sci. Technol.* **53**, 2695–2704 (2019).
- 571 39. Kim, C. *et al.* Ferrate promoted oxidative cleavage of sulfonamides: Kinetics and
572 product formation under acidic conditions. *Chem. Eng. J.* **279**, 307–316 (2015).
- 573 40. Zhang, H. *et al.* Enhanced ferrate(VI) oxidation of sulfamethoxazole in water by
574 CaO₂: The role of Fe(IV) and Fe(V). *J. Hazard. Mater.* **425**, 128045 (2022).
- 575 41. Luo, M. *et al.* Efficient activation of ferrate(VI) by colloid manganese dioxide:
576 Comprehensive elucidation of the surface-promoted mechanism. *Water Res.* **215**,
577 118243 (2022).
- 578 42. Tian, S.-Q., Wang, L., Liu, Y.-L. & Ma, J. Degradation of organic pollutants by
579 ferrate/biochar: Enhanced formation of strong intermediate oxidative iron species.
580 *Water Res.* **183**, 116054 (2020).
- 581 43. Yang, T. *et al.* UVA-LED-Assisted Activation of the Ferrate(VI) Process for
582 Enhanced Micropollutant Degradation: Important Role of Ferrate(IV) and Ferrate(V).
583 *Environ. Sci. Technol.* **56**, 1221–1232 (2022).
- 584 44. Lei, Y. *et al.* Assessing the Use of Probes and Quenchers for Understanding the
585 Reactive Species in Advanced Oxidation Processes. *Environ. Sci. Technol.* **57**, 5433–
586 5444 (2023).
- 587 45. Li, G. *et al.* Enhancing Ferrate Oxidation of Micropollutants via Inducing

588 Fe(V)/Fe(IV) Formation Needs Caution: Increased Conversion of Bromide to Bromate.
589 *Environ. Sci. Technol.* acs.est.3c01395 (2023) doi:10.1021/acs.est.3c01395.

590 46. Cheng, C., Chen, L., Chou, C. & Liang, J. Investigations of riboflavin photolysis
591 via coloured light in the nitro blue tetrazolium assay for superoxide dismutase activity.
592 *J. Photochem. Photobiol. B* **148**, 262–267 (2015).

593 47. Kono, Y. Reprint of: Generation of Superoxide Radical during Autoxidation of
594 Hydroxylamine and an Assay for Superoxide Dismutase. *Arch. Biochem. Biophys.* **726**,
595 109247 (2022).

596 48. Lee, H., Lee, C. & Kim, J.-H. Response to Comment on “Activation of Persulfate
597 by Graphitized Nanodiamonds for Removal of Organic Compounds”. *Environ. Sci.*
598 *Technol.* **51**, 5353–5354 (2017).

599 49. Huang, Z.-S. *et al.* Ferrate self-decomposition in water is also a self-activation
600 process: Role of Fe(V) species and enhancement with Fe(III) in methyl phenyl
601 sulfoxide oxidation by excess ferrate. *Water Res.* **197**, 117094 (2021).

602 50. Luo, C., Feng, M., Zhang, T., Sharma, V. K. & Huang, C.-H. Ferrate(VI) Oxidation
603 of Pharmaceuticals in Hydrolyzed Urine: Enhancement by Creatinine and the Role of
604 Fe(IV). *ACS EST Water* **1**, 969–979 (2021).

605 51. Sun, S. *et al.* Activation of ferrate by carbon nanotube for enhanced degradation of
606 bromophenols: Kinetics, products, and involvement of Fe(V)/Fe(IV). *Water Res.* **156**,
607 1–8 (2019).

608 52. Huang, Z.-S. *et al.* Impact of Phosphate on Ferrate Oxidation of Organic
609 Compounds: An Underestimated Oxidant. *Environ. Sci. Technol.* **52**, 13897–13907
610 (2018).

611 53. Qi, X. *et al.* Ferrate(VI) oxidation of substituted nitrobenzene compounds: Kinetics,
612 degradation, and oxidized products. *Chem. Eng. J.* **488**, 150921 (2024).

- 613 54. Zhang, H. *et al.* Different reaction mechanisms of $\text{SO}_4^{\bullet-}$ and $\bullet\text{OH}$ with organic
614 compound interpreted at molecular orbital level in Co(II)/peroxymonosulfate catalytic
615 activation system. *Water Res.* **229**, 119392 (2023).
- 616 55. Yang, C. *et al.* One-step synthesis of a 3D/2D $\text{Bi}_2\text{WO}_6/\text{g-C}_3\text{N}_4$ heterojunction for
617 effective photocatalytic degradation of atrazine: Kinetics, degradation mechanisms and
618 ecotoxicity. *Sep. Purif. Technol.* **288**, 120609 (2022).
- 619 56. Chen, X.-J. *et al.* pH-Driven Efficacy of the Ferrate(VI)–Peracetic Acid System in
620 Swift Sulfonamide Antibiotic Degradation: A Deep Dive into Active Species Evolution
621 and Mechanistic Insights. *Environ. Sci. Technol.* **57**, 20206–20218 (2023).
- 622 57. Deng, S. *et al.* Unveiling the activation mechanism: The role of nitrogen-doped
623 biochar in enhancing Fe(VI) catalysis. *Chem. Eng. J.* **486**, 150263 (2024).
- 624 58. He, F., Wang, J., Li, Y. & Sun, H. Quantum Chemistry Calculations on the
625 Mechanism of Isoquinoline Ring-Opening and Denitrogenation in Supercritical Water.
626 *Ind. Eng. Chem. Res.* **56**, 1782–1790 (2017).
- 627 59. Ogunsola, O. M. Decomposition of isoquinoline and quinoline by supercritical
628 water. *J. Hazard. Mater.* **74**, 187–195 (2000).
- 629 60. Zhang, Z. *et al.* Combining ferrate(VI) with thiosulfate to oxidize chloramphenicol:
630 Influencing factors and degradation mechanism. *J. Environ. Chem. Eng.* **9**, 104625
631 (2021).
- 632 61. Graham, N., Jiang, C., Li, X.-Z., Jiang, J.-Q. & Ma, J. The influence of pH on the
633 degradation of phenol and chlorophenols by potassium ferrate. *Chemosphere* **56**, 949–
634 956 (2004).
- 635 62. Xie, W. *et al.* Shale gas wastewater characterization: Comprehensive detection,
636 evaluation of valuable metals, and environmental risks of heavy metals and
637 radionuclides. *Water Res.* **220**, 118703 (2022).

- 638 63. Thompson, G. W., Ockerman, L. T. & Schreyer, J. M. Preparation and Purification
639 of Potassium Ferrate. VI. *J. Am. Chem. Soc.* **73**, 1379–1381 (1951).
- 640 64. Guo, B. *et al.* Enhanced Oxidation of Antibiotics by Ferrate Mediated with Natural
641 Organic Matter: Role of Phenolic Moieties. *Environ. Sci. Technol.* acs.est.3c03165
642 (2023) doi:10.1021/acs.est.3c03165.
- 643

644 **Acknowledgments**

645 This work was supported by the National Natural Science Foundation of China
646 (52070134, 52270075, 52300101), Sichuan University and Zigong City People's
647 Government Strategic Cooperation Project (2022CDZG-7), Litree Purifying
648 Technology Co., Ltd. Project (2021H012), and Sichuan University and Yibin City
649 People's Government strategic cooperation project (2020CDYB-2). A.T. acknowledges
650 the support of Politecnico di Torino. We would like to thank the Institute of New Energy
651 and Low-Carbon Technology, Sichuan University, for Raman tests. We would like to
652 thank the Analytical & Testing Center of Sichuan University for EPR measurement.

653

654 **Author information**

655 Authors and Affiliations

656 State Key Laboratory of Hydraulics and Mountain River Engineering, College of
657 Architecture and Environment, Institute for Disaster Management and Reconstruction,
658 Institute of New Energy and Low-Carbon Technology, Sichuan University, Chengdu,
659 Sichuan, 610207, China; Yibin Institute of Industrial Technology, Sichuan University
660 Yibin Park, Section 2, Lingang Ave., Cuiping District, Yibin, Sichuan, 644000, China

661 Ying Wang, Xin Chen, Liang Chen, Xin Cheng, Chunyan Yang, Guijing Chen, Jingyu
662 Shu & Baicang Liu

663 The Key Laboratory of Water and Sediment Sciences, Ministry of Education, College
664 of Environmental Sciences and Engineering, Peking University, Beijing 100871, China

665 Wen Liu

666 Department of Environment, Land and Infrastructure Engineering, Politecnico di
667 Torino, 10129, Turin, Italy

668 Alberto Tiraferri

669 Contributions

670 Ying Wang: Methodology, Investigation, Formal analysis, Writing – original draft. Xin

671 Chen: Data Curation, Software. Liang Chen: Software. Xin Cheng: Visualization,

672 Investigation. Chunyan Yang: Visualization, Investigation. Guijing Chen: Methodology,

673 Software. Jingyu Shu: Software. Wen Liu: Software. Alberto Tiraferri: Writing – review

674 & editing. Baicang Liu: Conceptualization, Supervision, Writing – review & editing.

675 Corresponding author

676 Correspondence to Baicang Liu

677

678 **Ethics declarations**

679 The authors declare that they have no known competing financial interests or

680 personal relationships that could have appeared to influence the work reported in this

681 paper.